Annals of Biomedical Engineering, Vol. 34, No. 9, September 2006 *(© 2006)* pp. 1414–1419
DOI: 10.1007/s10439-006-9115-7

Non-Invasive Determination of Zero-Pressure Geometry of Arterial Aneurysms

M. L. RAGHAVAN,[1] BAOSHUN MA,[1] and MARK. F. FILLINGER[2]

[1]Department of Biomedical Engineering, University of Iowa, Iowa City, IA and [2]Section of Vascular Surgery, Dartmouth Hitchcock Medical Center, Lebanon, NH

(Received 24 October 2005; accepted 15 March 2006; published online: 13 July 2006)

Abstract—Arterial aneurysms are in a pre-deformed state *in vivo* under non-zero pressure. The ability to determine their zero pressure geometry may help in improving accuracy of determination of stress distribution and reverse estimation of material properties from dynamic imaging data. An approximate method to recover the zero pressure geometry of the AAA is proposed. This method is motivated by the observation that the patterns in displacement field for a given AAA are strikingly consistent in an AAA under all physiological pressures. The basic principle is to leverage this observation to iteratively identify the geometry that when subjected to the *in vivo* pressure, will recover the geometry reconstructed from *in vivo* imaging. The methodology is demonstrated and validated using patient-specific AAA models.

Keywords—Aneurysm, Biomechanics, Finite element analysis.

INTRODUCTION

Estimation of stress distribution in patient-specific models of aortic and cerebral aneurysms has been proposed as a potentially useful indicator of rupture risk.[1–7] Reports on such stress analysis use geometry reconstructed from serial section diagnostic images of the aneurysms in their *in vivo* state. The reconstructed AAA wall surface is assumed to be stress free and subjected to uniform systolic pressure to determine the stress distribution. However in their *in vivo* state, aneurysms are not stress-free even if we ignore residual stress. Preferably, the zero-pressure configuration of the aneurysm must first be recovered and then the boundary conditions applied. Further, the advent of dynamic magnetic resonance imaging (dMRI) and gated computed tomography (gated-CT) offers the hope of patient-specific estimations of elastic properties. Alternatively, if the elastic properties are known to be reliable, temporal imaging data may be used for validation of the FE modeling. But for accomplishing such endeavors, the ability to recover the zero pressure configurations is indispensable. Here, we report on a methodology for approximately recovering the zero-pressure configuration of an aneurysm using geometry reconstructed from *in vivo* imaging.

Our goal is to use the *in vivo* aneurysm geometry (X_{im}) and luminal pressure (P_{im}) at the time of imaging to recover the zero-pressure geometry (X_0). In structures where residual stress is negligible and where the shape—not size—remains unchanged under deformation, this is quite straightforward even if its material is characterized by finite elastic models. Consider the case of a cell membrane under pressure, P_{im} whose known X_{im} and unknown X_0 are spherical. Both configurations can be fully described using a single variable, their radii—r_{im} and r_0. Clearly, r_0 is the radius of the sphere which when subjected to P_{im} will result in a deformed radius equal to r_{im}. r_0 is easily determined by iteratively subjecting spheres of different radii to pressure, P_{im} until the difference between the computed deformed radius and the known deformed radius (r_{im}) vanishes. This problem is solvable because the minimization process involved the estimation of just one variable, r_0. But what of structures whose geometry is not idealized and/or whose shape may change under deformations, such as patient-specific aneurysms? The above approach will not work because the geometry can only be described in a discretized form using numerous variables ($3 \times$ number of nodes) thus rendering the minimization problem intractable. However, we believe that the minimization problem is in fact solvable if we make some reasonable assumptions. Observations in this study suggest that there exists an underlying consistency in the deformation field of an arbitrarily shaped aneurysm wall irrespective of pressure applied. In this report, we describe this observation and leverage it to reduce the minimization problem to the estimation of just one variable allowing us to recover the zero-pressure configuration with a reasonable degree of accuracy.

METHODS

A human abdominal aortic aneurysm (AAA) wall surface reconstructed from CT data[8] and described by triangular elements (2048 nodes and 4054 elements) was used

Address correspondence to M. L. Raghavan, Department of Biomedical Engineering, University of Iowa, 1422 Seamans Center (SC), Iowa City, IA. Electronic mail: ml-raghavan@uiowa.edu

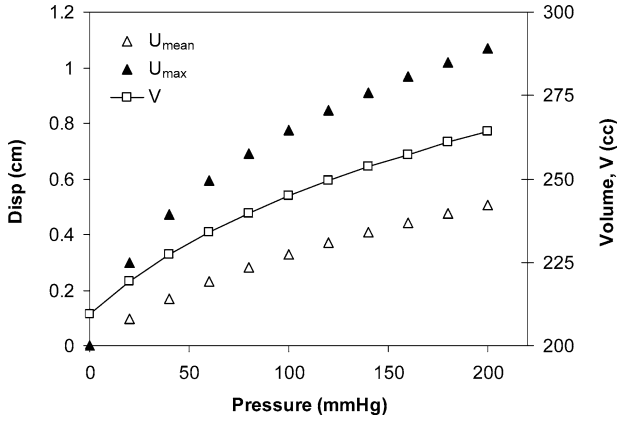

FIGURE 1. The variation in deformed lumen volume (V), surface averaged displacement magnitude (U_{mean}) and peak displacement magnitude (U_{max}) with pressure.

for demonstration of our observations on the nature of deformation field and validation of proposed methodology.

Observations on the Consistency of the Deformation Field

For purposes of demonstration alone, the reconstructed AAA wall surface was assumed to be truly at zero pressure. A previously reported isotropic finite elastic material model with population mean material parameters[9] was used to describe elastic behavior. The nodes at the proximal aorta and distal iliac artery edges were constrained from displacement in all directions. Using the finite element (FE) method in ABAQUS, the AAA wall was individually subjected to quasi-static pressures from 20 through 200 mmHg (increments of 20 mmHg) and the resulting displacement field for each increment of pressure determined as reported earlier.[7] Figure 1 shows the variation in deformed lumen volume, surface averaged displacement magnitude and peak displacement magnitude with pressure. All values reported in this report are for the mid-surface within the shell thickness. As should be expected, the AAA becomes progressively less compliant with increasing pressure. Interestingly however, the *pattern* of displacement magnitude and the direction of the displacement vector changes little between different pressures. To study this quantitatively, the normalized displacement magnitude field (U_n) was calculated. For a given node, the normalized displacement magnitude U_n is given by

$$U_n = U/U_{max}$$

where, U is the computed displacement magnitude at the node and U_{max}, the maximum U of all nodes in the AAA model for a given pressure. U_n varies from 0 to 1. Figure 2 demonstrates the remarkable similarity in U_n induced by pressures of 20, 60, 120 and 200 mmHg in. Further, there is little change in the direction of the displacement vector

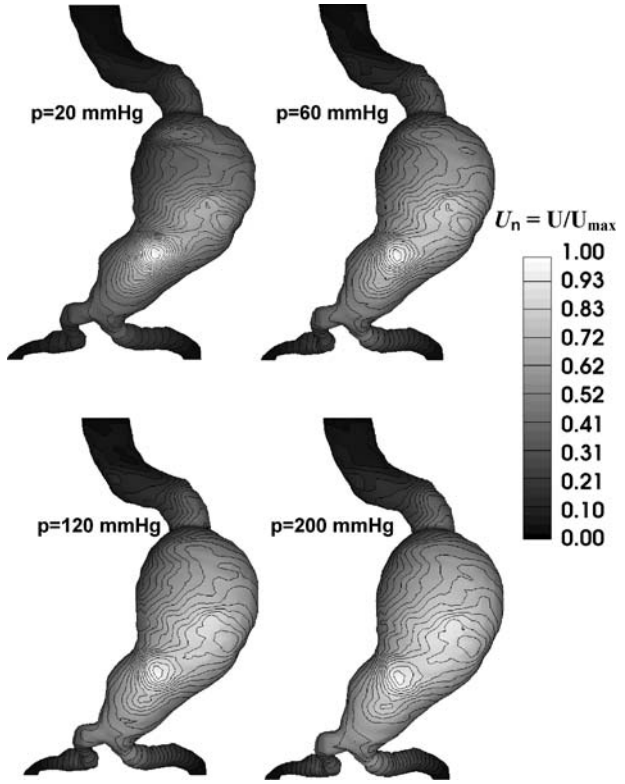

FIGURE 2. Distribution of normalized displacement magnitude, U_n. Note that significant increase in luminal pressure causes minimal change in U_n distribution. All images are to scale.

within the range of pressures applied. That is, the entire path of each node in the AAA surface under pressures ranging from 0 through 200 mmHg may be reliably approximated by straight line. Parametric straight line fits (i.e., x-position vs. arc length; y-position vs. arc length and z-position vs. arc length) were generated for the path taken by each node in the AAA surface as pressure varied from 0 to 200 mmHg. R^2 values averaged across all nodes were 0.89, 0.97, and 0.95 respectively for X, Y and Z. Taken together, they support the following approximations:

1. the unit displacement vector (i.e., direction) field in an AAA surface under any physiological pressure P_1 is the same as that under any other physiological pressure P_2;
2. the displacement magnitude field under P_1 differs from the displacement magnitude field under P_2 only by a single multiplication factor.

These assumptions form the basis for the development of a method for approximately recovering the zero pressure geometry from *in vivo* geometry. An alternative way to look at the implications of our observations is this: AAA deformation under pressure may be thought of as two separate parts—the change in shape and the change in size.

Figure 2 essentially demonstrates that the change in shape, although can only be described by numerous quantities—$U_n(x,y,z)$—is actually quite consistent between increments of pressure. Consequently, if we know the change in shape for any one increment of pressure, we can safely assume it to be the same for any given increment of pressure. The change in size on the other hand is governed by the nonlinearity of the stress-strain curve (or more precisely, the chosen constitutive model), but this is described by a single quantity (any size-change measure such as U_{max}) and may therefore be obtained by a minimization routine. This precisely is the underlying rationale of our proposed approach.

Proposed Methodology for Recovery of Zero Pressure Geometry

In this section, X is used to denote an $n \times 3$ array (x, y, and z coordinate values of n nodes describing a triangulated surface). The element connectivities remain the same during transformations and therefore, X may itself be used to uniquely describe a given geometry. x is used to denote the FE-computed deformed geometry when X is subjected to luminal pressure. The goal is to determine the candidate zero pressure geometry (X_{0-pred}) which when subjected to the known luminal pressure at imaging (P_{im}) will result in a deformed geometry (x_{0-pred}) that is closest to the known *in vivo* geometry during imaging (X_{im}). At the outset, this is an ill-posed problem because X_{0-pred} is described by 3n variables and optimizing for so many variables is an impossible task. But as postulated earlier, if the displacement field may be known for any one pressure applied to any single configuration (the shape-change measure), then determination of a multiplication factor alone (the size-change measure) may be sufficient to recover X_{0-pred}. This is the premise of the proposed methodology illustrated schematically in Fig. 3. Briefly, the basic approach is to first determine one such displacement field (U) by applying P_{im} to X_{im} assuming it to be stress free. Then this displacement field is scaled by a multiplication factor, $-k$ and applied to X_{im} to obtain a shrunk geometry (X_{0k}). X_{0k} is then subjected to P_{im} and the resulting deformed geometry (x_{0k}) determined. The sum of square difference between x_{0k} and the known X_{im} is calculated (E_{obj}). The process is repeated for multiple values of k until a minima in E_{obj} is found. The X_{0k} for which E_{obj} is minimized is the predicted zero pressure geometry. The objective function E is a measure of the difference between two geometries. It is the square of the displacement magnitude field that transforms one geometry into the other summed over all nodes.

Mean aortic pressure is recommended as P_{im} for patient-specific AAA reconstructed from routine non-gated abdominal CT data. Such scanning spans the entire length of the AAA in about 10–20 sec. The sectional slices therefore come from different stages of the cardiac cycle. Nevertheless, since AAA undergoes minimal pulsation (2–5% in diameter[10]), the reconstructed and smoothed geometry may be thought of as being under mean aortic pressure. If routine imaging becomes more stringent in the future (e.g., use of dynamic CT) allowing for diastole- or systole-specific imaging, then P_{im} may be P_{sys} or $P_{diastolic}$ as the case may be.

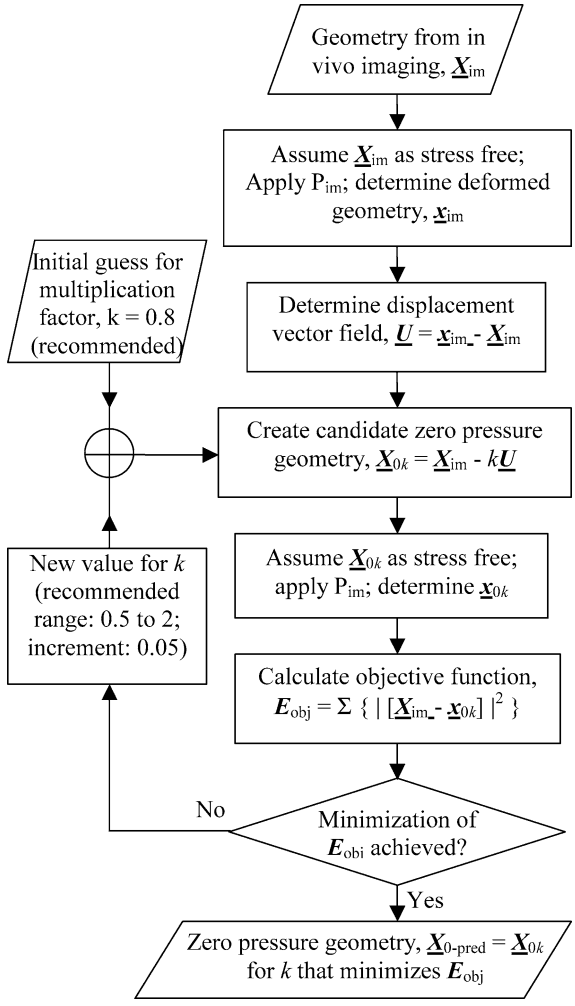

FIGURE 3. Flow chart of proposed methodology for recovering zero pressure geometry.

Validation

The accuracy of the proposed methodology was investigated using multiple realistic AAA models. First, the 3D model was taken to be truly under zero pressure (X_0) with material model and proximal/distal constraints as described in the earlier section. The equivalent of the image-reconstructed 3D model, X_{im} is obtained by subjecting X_0 to P_{im}. It is this X_{im} that is now available to the user. Our goal here is to start with X_{im}, use the proposed methodology to predict the zero pressure geometry (X_{0-pred}) and then

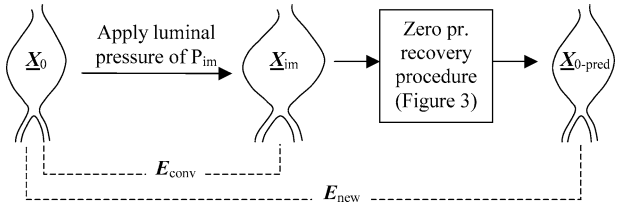

FIGURE 4. Validation procedure used. The process between X_{im} and X_{0-pred} was blinded from the process between X_0 and X_{im}.

compare it to the known zero pressure geometry (X_0). Figure 4 illustrates the verification method graphically. The sum of square error function, E_{new} is used to quantify the difference between X_{0-pred} and X_0. In order to place E_{new} in context, the error in the conventional approach, E_{conv}—defined as the sum of square difference between X_0 and X_{im}—is also calculated.

$$E_{new} = \Sigma\{|\underline{X}_{0\text{-pred}} - \underline{X}_0|^2\}, \qquad E_{conv} = \Sigma\{|\underline{X}_{im} - \underline{X}_0|^2\}$$

Three cases were studied for the validation procedure. In case 1, the AAA used in earlier section was assumed to have P_{im} of 100 mmHg. In case 2, this same AAA was assumed to be from a severely hypertensive patient with a P_{im} of 180 mmHg. In case 3, a different AAA model was assumed to have P_{im} of 100 mmHg. Figure 5 shows the k vs E_{obj} relationship for these cases. Optimal value for k ranged between 0.95 and 1. Figure 6 shows graphical comparisons between X_0, X_{im} and X_{0-pred} for the severely hypertensive case. Table 1 lists the error measures for all cases. Results of the validation study show that the proposed methodology helped to recover the zero pressure geometry to a reasonable degree of accuracy. The error in predicting the zero pressure geometry with the use of the proposed methodology (E_{new}) appears to be a small fraction of the error in the conventional approach (E_{conv}), but even so, it is still only an approximation. And finally, we also computed the stress distributions using the conventional and proposed approaches for all 3 cases (see Fig. 5). The peak von Mises wall stress between the conventional and proposed approaches were 27.1 vs. 26.9 N/cm^2 for case 1 (0.7% error), 54.0 vs. 52.6 N/cm^2 for case 2 (2.7% error) and 22.8 vs. 22.4 N/cm^2 for case 3 (1.8% error). Clearly, this suggests that the assumption in the conventional approach on zero pressure geometry is reasonable, as long as the goal is confined to computation of stress distribution. Increasing hypertension is likely to increase this error. But the fact that the stresses aren't significantly different in the cases studied is understandable because spatially high stresses may be more sensitive to shape differences than size changes. However, when the change in size becomes an important part of the problem such as during inverse-FE based parameter estimation from temporal image data (e.g., dMRI or gated-CT), then the recovery of zero pressure configuration becomes indispensable.

DISCUSSION

A methodology to recover the zero pressure geometry of aneurysms has been proposed. The underlying rationale is that the shape change in an AAA is consistent and may be approximately recovered. The size change under pressure can then be determined accurately using an error minimization routine. The validation study with multiple realistic AAA models demonstrated that the recovered zero pressure geometry is likely a reasonable approximation. The ability to recover the zero pressure geometry may only slightly improve estimations of stress distribution, but can facilitate validation of FE analyses[11] and allow for material property estimations from *in vivo* dynamic imaging. It has to be noted that the method depends on other modeling choices

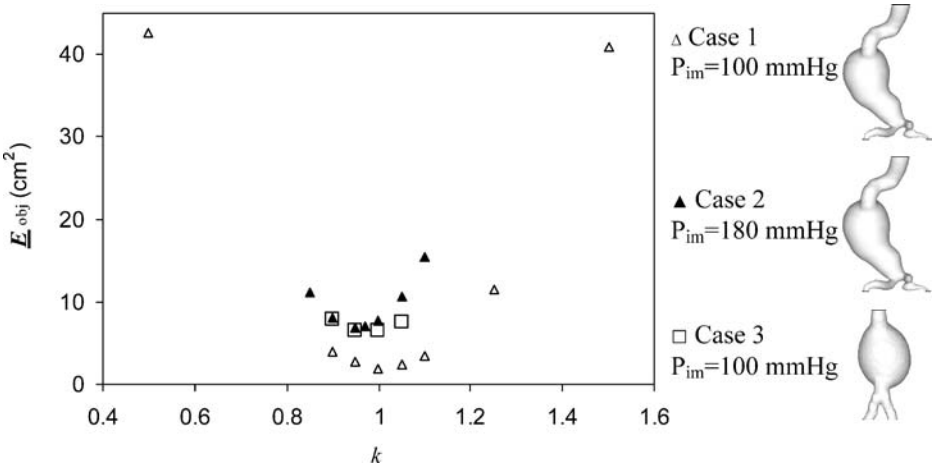

FIGURE 5. Minimization of objective function for the three cases studied. The optimal k varied between 0.95 and 1.0 in these cases. The morphology of AAA models shown are to scale. Further details on the three cases are provided in Table 1.

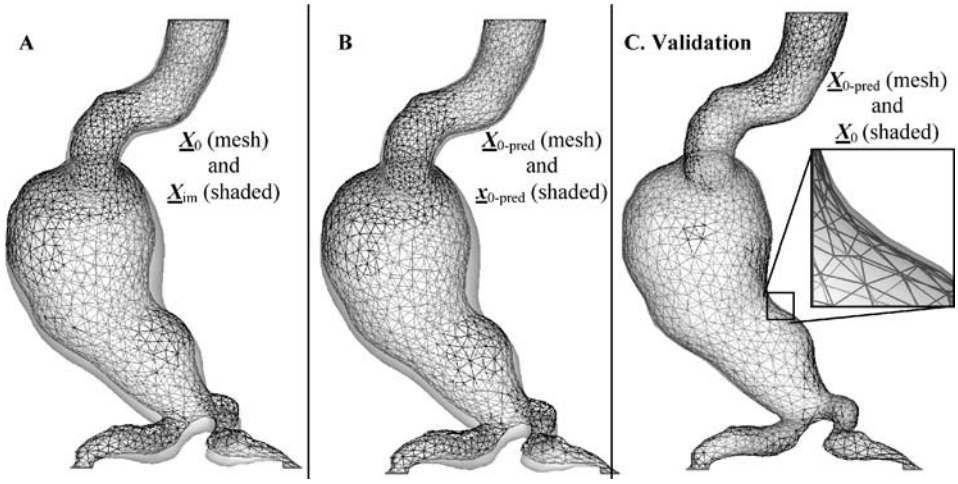

FIGURE 6. Comparison of geometries from validation procedure. All images are to scale. The difference between the recovered and true zero pressure geometries (C) is quite small and may only be perceived in the zoomed insert (12 × magnification).

being reasonable such as the material model and boundary conditions. Limitations in this approach are worth noting. It has been assumed that residual stresses if present are negligible in the aneurysmal wall. Unreported observations by our group support this premise, but additional studies are needed. All reported studies in AAA biomechanics have ignored residual stress.[1–6,8] We studied whether this method will work when anisotropic material models are employed. We used a patient-specific cerebral aneurysm model described by a Fung-type constitutive law.[12] Following the validation protocols, we found that the E_{obj} was minimized at $k = 1.00$ with E_{new}/E_{conv} ratio (error in zero pressure geometry from proposed method as a fraction of error in conventional approach) was 12.74%, suggesting that this method may work well for anisotropic models and at smaller size scales as well. We also studied whether this method will work for AAA walls with regionally varying wall thickness. An AAA model with regionally varying wall thickness (based on experimental measurements) was studied according to the validation protocol in Fig. 4. We found the E_{obj} was minimized at $k = 0.90$ with E_{new}/E_{conv} ratio of 23.83% suggesting that the method may be less reliable when AAA have regionally variable thickness. Essentially, the underlying premise of this approach is based in heuristics, not theory. Therefore, when the computational model differs significantly from that demonstrated here (e.g., use of solid 3D element types and incorporation of intra-luminal thrombus or vertebral constraints into FE model), additional validation is recommended. Our group recently reported a theoretically sound method of recovering the zero pressure geometry using inverse elastostatics where the spatial form of equilibrium equation is used and the Cauchy stress parameterized in terms of an inverse deformation gradient.[13] That approach is superior to the one proposed here, but requires modifications to FE solution schemes and impossible with current commercial solvers. The current proposed method offers an alternative first order approximation of the zero pressure geometry and is easily performed using commercial FE solvers.

TABLE 1. Results from validation procedure for the three cases studied (see Fig. 5 for morphology of the AAA models used).

Case #	P_{im} (mmHg)	Minimum E_{obj} (cm^2)	Optimal k	E_{conv} (cm^2)	E_{new} (cm^2)	E_{new}/E_{conv}
1 (AAA#1)	100	1.97	1.00	202.40	5.57	2.75%
2 (AAA#1)	180	6.95	0.95	426.31	16.35	3.84%
3 (AAA#2)	100	6.48	1.00	293.95	29.84	10.15%

ACKNOWLEDGMENTS

This study was supported in part by NHLBI NIH R01 HL64351-01: The Role Of Wall Stress Distribution In Abdominal Aortic Aneurysms (to MFF).

REFERENCES

[1]Di Martino, E. S., G. Guadagni, A. Fumero, G. Ballerini, R. Spirito, P. Biglioli, and A. Redaelli. Fluid-structure interaction within realistic three-dimensional models of the aneurysmatic aorta as a guidance to assess the risk of rupture of the aneurysm. *Med. Eng. Phys.* 23(9):647–55, 2001.

[2]Fillinger, M. F., S. P. Marra, M. L. Raghavan, and F. E. Kennedy. Prediction of rupture risk in abdominal aortic aneurysm during observation: Wall stress versus diameter. *J. Vasc. Surg.* 37(4):724–32, 2003.

[3]Fillinger, M. F., M. L. Raghavan, S. P. Marra, J. L. Cronenwett, and F. E. Kennedy. *in vivo* analysis of mechanical

wall stress and abdominal aortic aneurysm rupture risk. *J. Vasc. Surg.* 36(3):589–97, 2002.

[4]Raghavan, M. L., D. A. Vorp, M. P. Federle, M. S. Makaroun, and M. W. Webster. Wall stress distribution on three-dimensionally reconstructed models of human abdominal aortic aneurysm. *J. Vasc. Surg.* 31(4):760–9, 2000.

[5]Thubrikar, M. J., J. al-Soudi, and F. Robicsek. Wall stress studies of abdominal aortic aneurysm in a clinical model. *Ann. Vasc. Surg.* 15(3):355–66, 2001.

[6]Wang, D. H., M. S. Makaroun, M. W. Webster, and D. A. Vorp. Effect of intraluminal thrombus on wall stress in patient-specific models of abdominal aortic aneurysm. *J. Vasc. Surg.* 36(3):1–7, 2002.

[7]Raghavan, M. L., M. F. Fillinger, S. P. Marra, B. P. Naegelein, and F. E. Kennedy. Automated methodology for determination of stress distribution in human abdominal aortic aneurysm. *J. Biomech. Eng.* 127(5):868–71, 2005.

[8]Raghavan, M. L., M. F. Fillinger, S. P. Marra, B. P. Naegelein, and F. E. Kennedy. Automated methodology for determination of stress distribution in human abdominal aortic aneurysm. *J. Biomech. Eng.* in press, 2005.

[9]Raghavan, M. L. and D. A. Vorp. Toward a biomechanical tool to evaluate rupture potential of abdominal aortic aneurysm: Identification of a finite strain constitutive model and evaluation of its applicability. *J. Biomech.* 33(4):475–82, 2000.

[10]Vorp, D. A., W. A. Mandarino, M. W. Webster, and J. Gorcsan, Third potential influence of intraluminal thrombus on abdominal aortic aneurysm as assessed by a new non-invasive method. *Cardiovasc. Surg.* 4(6):732–9, 1996.

[11]Marra, S. P., M. L. Raghavan, D. R. Whittaker, M. F. Fillinger, D. Chen, J. M. Dwyer, M. J. Tsapakos, and F. E. Kennedy. Estimation of the zero-pressure geometry of abdomimal aortic aneurysms from dynamic magnetic resonance imaging. in 2005 Summer Bioengineering Conference. 2005. Vail, CO.

[12]Ma, B., J. Lu, R. E. Harbaugh, and M. L. Raghavan. Modeling the geometry, hemodynamics and tissue mechanics of cerebral aneurysms. in 2004 ASME International Mechanical Engineering Congress and Exposition. 2004. Anaheim, CA.

[13]Lu, J., X. Zhou, and M. L. Raghavan. Inverse Elastostatic Stress Analysis in Pre-deformed Biological Structures: Demonstration Using Abdominal Aortic Aneurysms. *J Biomech*, in press, 2006.